



# Magnetic field annealing dependent magnetic properties of $\text{Co}_{90}\text{Pt}_{10}$ nanowire arrays

S. Shamaila, R. Sharif, J.Y. Chen, H.R. Liu, X.F. Han\*

Beijing National Laboratory for Condensed Matter Physics, Institute of Physics, Chinese Academy of Science, Beijing 100190, China

## ARTICLE INFO

### Article history:

Received 9 January 2009

Received in revised form

15 April 2009

Available online 13 August 2009

### Keywords:

Magnetic field annealing

Magnetic anisotropy

CoPt nanowires

### PACS:

75.75.+a

75.60.Nt

75.50.-y

## ABSTRACT

$\text{Co}_{90}\text{Pt}_{10}$  alloy and elemental Co nanowires (NWs) are fabricated by electrodeposition in the self-assembled anodic alumina templates. The fabricated NWs are subjected to magnetic field (MF) annealing under 1000 Oe applied magnetic field in a direction parallel to the nanowire axis at 265 °C. The corresponding changes in the saturation magnetization, coercivity, remanent squareness, the shape of hysteresis loops and crystal structure of NWs before and after MF annealing have been investigated. The enhanced magnetic anisotropy has been observed in  $\text{Co}_{90}\text{Pt}_{10}$  alloy NWs by MF annealing. The elemental Co NWs have not been affected by MF annealing. The stress relief between the domains and diffusional pair ordering of unlike atoms along the direction of external applied field are thought to be the causes of enhanced anisotropy. Re-annealing of the samples in the absence of magnetic field at 600 °C does not completely remove the enhanced anisotropy. The shape of the NWs is concluded to play major role in persistence of enhanced magnetic anisotropy after high temperature reannealing.

© 2009 Elsevier B.V. All rights reserved.

## 1. Introduction

Miniaturization of advanced devices, such as sensors and micromotors, requires the development of nanostructures. Intensive efforts have been devoted in the development of nanostructures to attain the combined goals of a high areal density of bits and adequate thermal stability [1]. Cobalt alloys, and in particular cobalt platinum alloys are considered as a very promising candidate for such applications and specially for perpendicular magnetic recording [2–5]. An alloy composed of two kinds of materials is expected to produce a fine new magnetic material that has both high magnetization and coercivity. Template assisted magnetic nanowire arrays, in principle, present an attractive potential medium because the fabricated nanowires (NWs) by electrodepositing transitional metals or their alloys into the nanopores of the templates comprise a highly ordered pattern of reasonably magnetically isolated units [1]. Ferromagnetic NWs exhibit unique and tunable magnetic properties due to the inherent shape anisotropy and the small wire dimensions [6,7]. The material microstructure, grain size and crystallite orientations play an important role in magnetic properties of NWs such as hysteresis and remanent magnetization [8,9]. These microstructural features, in turn, are determined by the conditions under which the material is prepared and treated [10,11]. The controlled

variations in magnetic properties of NWs in accordance with the practical applications are an attractive topic in field of magnetic devices. The intrinsic properties of materials such as magnetic anisotropy (MA) and magnetostriction have been investigated for long time [12]. Especially the modeling of anisotropy is of technological interest since it can broaden the applications of materials in devices. Researchers have described the application of magnetic field (MF) during electrochemical growth of magnetic NW arrays with an attempt to study its influence on their structural and magnetic properties [13–15]. MF annealing is an established technique for inducing a magnetic anisotropy in both crystalline and amorphous materials [16–19]. Currently, there are limited reports on systematic investigations of enhanced magnetic anisotropy for electrodeposited ferromagnetic NWs. In the present report, elemental (Co) and alloy ( $\text{Co}_{90}\text{Pt}_{10}$ ) nanowire (NW) arrays are prepared by AC electrodeposition into nanochannels of porous alumina membranes. The crystal structure, magnetic and magnetization properties of the nanowires (NWs) have been studied. For detailed analysis,  $\text{Co}_{90}\text{Pt}_{10}$  and Co NWs are subjected to magnetic field (MF) annealing and reannealing (without field) at higher temperature. An enhanced magnetic anisotropy (MA) and a large increase in saturation magnetization ( $M_s$ ) in case of  $\text{Co}_{90}\text{Pt}_{10}$  alloy NWs have been evidenced by the changes in hysteresis loops of the samples before and after MF annealing processes. Post deposition MF annealing does not affect the properties of elemental Co NWs although magnetic field has some effects on such NWs when it is applied during the growth of NWs [13–15].

\* Corresponding author.

E-mail address: [xfhan@aphy.iph.ac.cn](mailto:xfhan@aphy.iph.ac.cn) (X.F. Han).

## 2. Experimental

The high purity (99.99%) aluminum (Al) foil was ultrasonically degreased in trichloroethylene for 5 min, and etched in 1.0M NaOH for 3 min at room temperature (RT). It was then electro-polished in a mixed solution of  $\text{HClO}_4 : \text{CH}_3\text{CH}_2\text{OH} = 1 : 4$  (by volume) for 3 min with a constant potential of about 12 volts (V). To obtain highly ordered pores, a two-step anodization was used. In the first anodization step the Al foil was anodized at  $0^\circ\text{C}$  and 40V dc in 0.3M oxalic acid for about 12 h to form textures on Al surface. The formed aluminum oxide layer was then removed by immersing anodized Al into a mixed solution of 0.4M chromic acid and 0.6M phosphoric acid solution at  $60^\circ\text{C}$ . Subsequently, the samples were reanodized for 8 h under the same anodization conditions as in the first step. A nonequilibrium anodization process in which the voltage was reduced to about 8V followed the second anodization. This led to a reduction of the barrier layer that formed between the porous alumina and the Al substrate, thus facilitating the electrodeposition of the metals. These self-assembled anodic aluminum oxide (AAO) templates were used to fabricate  $\text{Co}_{90}\text{Pt}_{10}$  and Co NW arrays by AC-electrochemical deposition method. The electrolyte contained  $\text{PtCl}_4$ ,  $\text{CoSO}_4 \cdot 7\text{H}_2\text{O}$ , and  $\text{H}_3\text{BO}_3$  for  $\text{Co}_{90}\text{Pt}_{10}$  NWs and  $\text{CoSO}_4 \cdot 7\text{H}_2\text{O}$ , and  $\text{H}_3\text{BO}_3$  for Co NWs. The pH of both solutions was kept to about 3.0 to get fcc structured NWs [20]. The AC-deposition was conducted with a sinusoidal voltage, using a standard double electrode bath, the AAO template was used as one electrode, and the platinum wire was used as another. The MF annealing of the samples was carried

out under 1000 Oe magnetic field applied parallel to the nanowire axis at  $265^\circ\text{C}$  for 2 h. The samples were re-annealed without magnetic field at  $600^\circ\text{C}$  for  $\frac{1}{2}$ h. For comparison as deposited  $\text{Co}_{90}\text{Pt}_{10}$  NWs were also annealed in zero magnetic field at  $500^\circ\text{C}$ . X-ray diffraction (XRD) was performed to analyze the crystal structure of the NWs. Atomic force microscopy (AFM), transmission electron microscopy (TEM) and field emission scanning electron microscopy (FESEM) were used to characterize the morphology and size of the templates and NWs. The contents of the NWs were determined using induction coupled plasma spectrometry (ICP). The analysis disclosed that the composition of individual sample is almost homogeneous. The magnetic properties of the same samples before, after annealing with and without MF and then reannealing process are investigated using vibrating sample magnetometry (VSM).

## 3. Results and discussion

Fig. 1 shows (a) AFM top view ( $1 \times 1 \mu\text{m}^2$ ), (b) AFM top view ( $0.5 \times 0.5 \mu\text{m}^2$ ) and (c) three-dimensional AFM image ( $1 \times 1 \mu\text{m}^2$ ) of the surface topography of nanopore array in anodic alumina prepared by two-step anodization. Uniform pores with an average pore diameter of about 40 nm and center-to-center spacing of about 100 nm have been obtained. The fabricated AAO templates contain self-assembled pore arrays with quasihexagonal ordering. Generally, pore diameter of AAO film is increased if the anodized voltage is large, and length of the pores is increased with time for anodization.

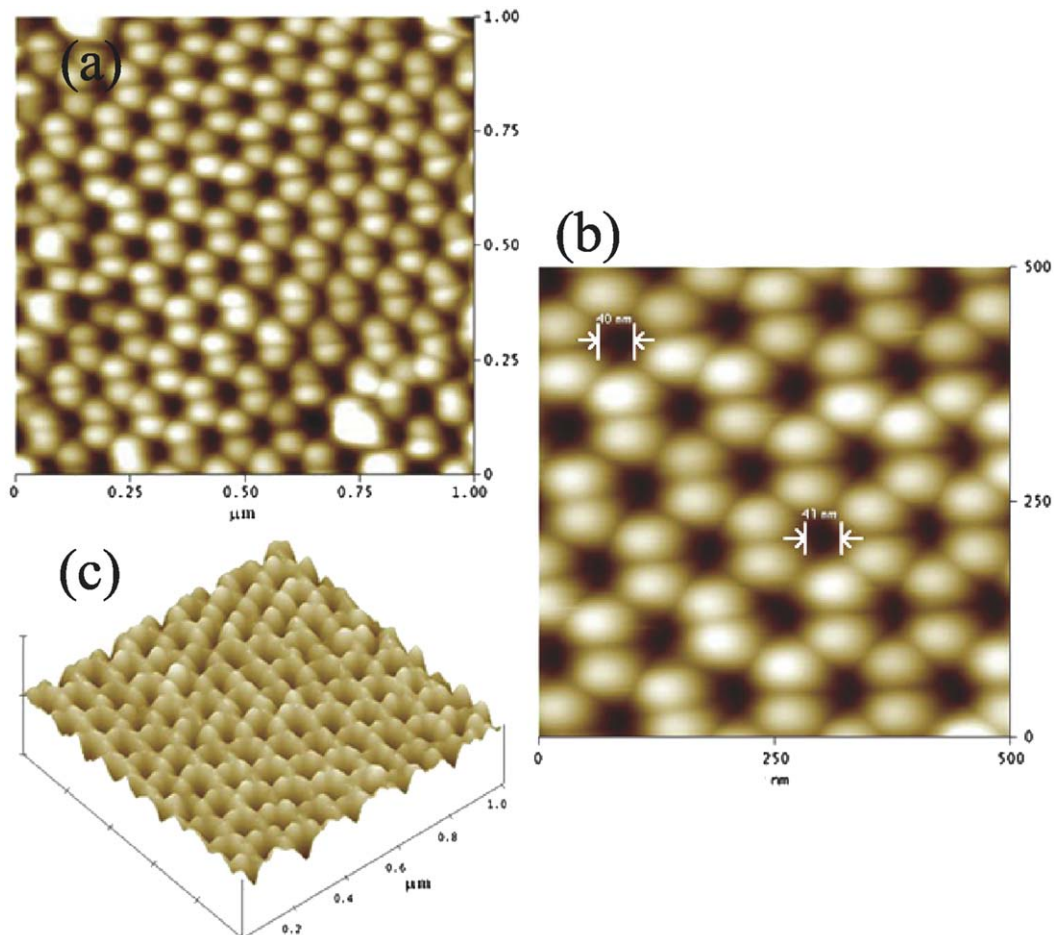


**Fig. 1.** (a) AFM top view ( $1 \times 1 \mu\text{m}^2$ ), (b) AFM top view ( $0.5 \times 0.5 \mu\text{m}^2$ ) and (c) three-dimensional AFM image ( $1 \times 1 \mu\text{m}^2$ ) of the surface topography of nanopore array in anodic alumina prepared by two-step anodization.

Fig. 2 presents some typical TEM images of (a)  $\text{Co}_{90}\text{Pt}_{10}$  alloy NWs and (b) Co NWs liberated from AAO template by immersion in an aqueous 1 M NaOH solution. The average diameter of the NWs are about 40 nm, in agreement with that of the pores in the AAO template. The lengths of  $\text{Co}_{90}\text{Pt}_{10}$  and Co NWs observed by FESEM before dissolving the membrane are found to be about 15 and 20  $\mu\text{m}$ , respectively.

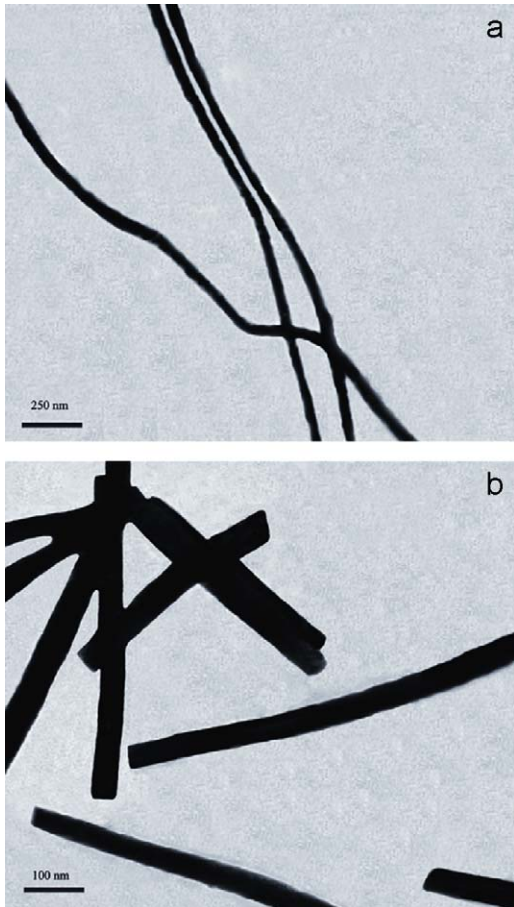


Fig. 2. TEM images of isolated (a) CoPt nanowires and (b) Co nanowires liberated from AAO template by dissolving the alumina layer with NaOH aqueous solution.

The magnetic field annealing effects on the magnetic properties of  $\text{Co}_{90}\text{Pt}_{10}$  NW arrays are described in Fig. 3(a–c). The inset of Fig. 3c shows the variations in saturation magnetization ( $M_s$ ) of  $\text{Co}_{90}\text{Pt}_{10}$  NW arrays. After MF annealing a large increase in the  $M_s$  along with modest variations in magnetic properties indicates that the magnetic anisotropy has been enhanced in  $\text{Co}_{90}\text{Pt}_{10}$  alloy NWs. The magnetic anisotropy constant ( $K_u$ ) calculated for  $\text{Co}_{90}\text{Pt}_{10}$  alloy NWs is found to be increased from  $3.76 \pm 0.5 \times 10^5$  to  $8.66 \pm 0.5 \times 10^5 \text{ J/m}^3$  after MF annealing. The origin of this enhanced magnetic anisotropy (MA) is the atomic pair ordering of Co and Pt atoms and relief of stress between the grains.

The strength of the field induced anisotropy ( $K_u$ ) in a binary alloy like  $\text{Co}_{1-x}\text{Pt}_x$  varies as

$$K_u \propto \frac{1}{k_B T_a} \left[ \frac{M_s(T_a)}{M_s(0)} \right]^2 \left[ \frac{M_s(T)}{M_s(0)} \right]^2 x^2 (1-x)^2 \quad (1)$$

where  $k_B$  is the Boltzmann constant,  $T_a$  is the annealing temperature and  $x$  represents the contents of elements in the alloy system [12]. This expression describes the relation of  $K_u$  with alloy composition as  $x^2(1-x)^2$ , saturation magnetization after annealing ( $M_s(T_a)$ ), annealing temperature ( $T_a$ ) and saturation magnetization at measurement temperature ( $M_s(T)$ ). For same annealing and measurement temperature, the  $K_u$  will be determined from the composition of alloy and  $M_s(T_a)$ . Furthermore for a particular composition  $K_u$  will be proportional to the square of  $M_s(T_a)$ . This trend is in agreement with the observed results for  $\text{Co}_{90}\text{Pt}_{10}$  alloy NWs and calculated values of  $K_u$  from the experimental  $M$ – $H$  curves obtained with the field applied in both directions.

As a reference, NW arrays of elemental Co are also subjected to MF annealing and  $M$ – $H$  curves of Co NW arrays as deposited, after MF annealing and after reannealing are shown in Fig. 4(a–c). The inset of Fig. 4(c) shows that there is no change in the  $M_s$  of Co NWs. The phenomenon of enhanced MA does not appear in case of pure elements [12] as in the present case NWs of pure Co do not respond to the MF annealing treatment.

The variations in the values of magnetic parameters, coercivity ( $H_c$ ) and remanent squareness ( $SQ$ ) with field applied in parallel and perpendicular to the NW axis are summarized in Tables 1 and 2 for  $\text{Co}_{90}\text{Pt}_{10}$  and Co NWs, respectively. Comparison of the parameters in Table 1 indicates that after MF annealing there is an increase in the values of  $H_c$  with small changes in  $SQ(M_r/M_s)$  of  $\text{Co}_{90}\text{Pt}_{10}$  NW arrays resulting in the enhancement of magnetic anisotropy of alloy NWs. Table 2 presents that the changes in

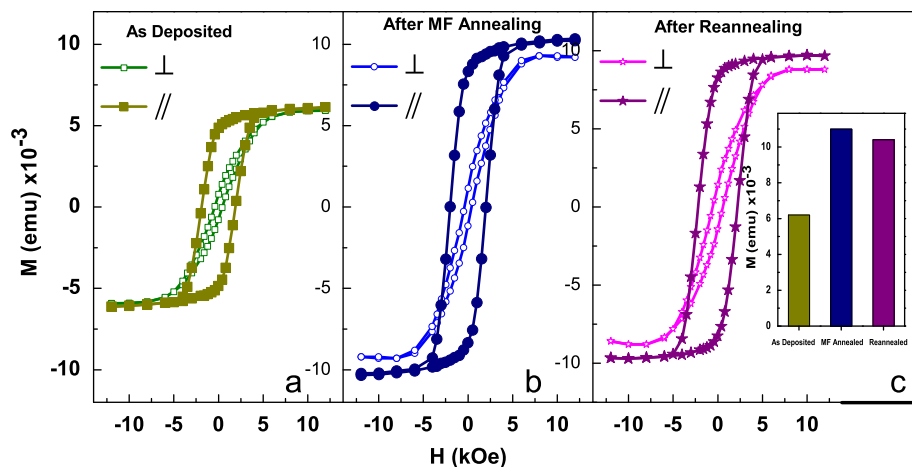
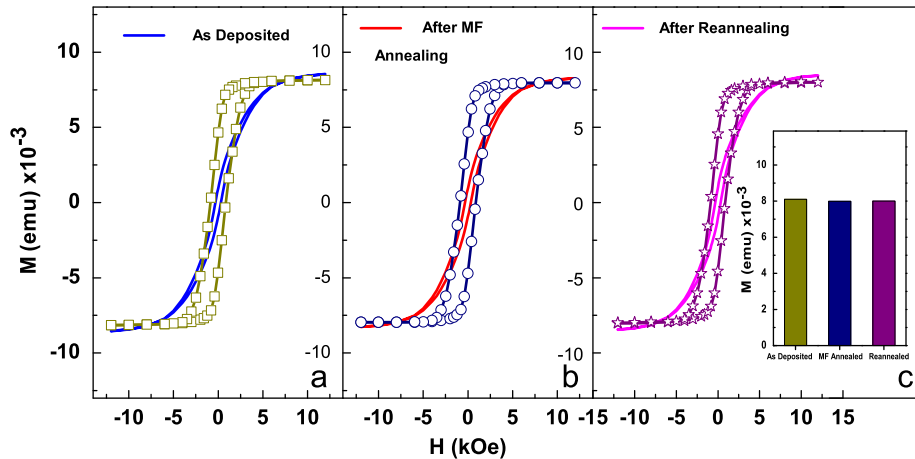


Fig. 3. Magnetic hysteresis curves of  $\text{Co}_{90}\text{Pt}_{10}$  alloy nanowire arrays measured with magnetic field applied parallel and perpendicular to the nanowire axis (a) as deposited, (b) after MF annealing and (c) after reannealing process, the inset shows the variations in saturation magnetization after the annealing processes.



**Fig. 4.** Magnetic hysteresis curves of Co nanowire arrays measured with the magnetic field applied parallel and perpendicular to the nanowire axis (a) as deposited, (b) after MF annealing and (c) after reannealing process, the inset shows the variations in saturation magnetization after the annealing processes.

**Table 1**

The variations in the magnetic properties of  $\text{Co}_{90}\text{Pt}_{10}$  alloy nanowire arrays due to the MF annealing process.

Magnetic parameters	$\text{Co}_{90}\text{Pt}_{10}$		
	As deposited	MF annealing	Reannealing
$H_{c\parallel}(\text{Oe})$	1907	2033	2188
$H_{c\perp}(\text{Oe})$	359	371	527
$SQ_{\parallel}(M_r/M_s)$	0.80	0.83	0.87
$SQ_{\perp}(M_r/M_s)$	0.16	0.15	0.17

**Table 2**

The variations in the magnetic properties of Co nanowire arrays due to the MF annealing process.

Magnetic parameters	Co		
	As deposited	MF annealing	Reannealing
$H_{c\parallel}(\text{Oe})$	864	888	877
$H_{c\perp}(\text{Oe})$	300	316	323
$SQ_{\parallel}(M_r/M_s)$	0.57	0.59	0.57
$SQ_{\perp}(M_r/M_s)$	0.11	0.12	0.12

magnetic parameters for Co NWs are negligible as compare to that of  $\text{Co}_{90}\text{Pt}_{10}$  NWs.

The magnetization behavior of the  $\text{Co}_{90}\text{Pt}_{10}$  NWs can be explained according to the model of prolate ellipsoid chains [21]. According to the model, the coercivity of the nanowires can be written as

$$H_c = [\pi(6M_n + 2L_n)a^2M_s/(6b^2)] + [4\pi(N_{\perp} - N_{\parallel})M_s] \quad (2)$$

where

$$M_n = \sum_{j=1}^{(n-2)/2 < j \leq n/2} [(n-2j)/[n(2j)^3]]$$

$$L_n = \sum_{j=1}^{(n-1)/2 < j \leq (n+1)/2} [n - (2j - 1)]/[n(2j - 1)^3]$$

$n$  is the number of ellipsoids in one wire,  $a$  is the length of short axis of the ellipsoid and diameter of the NWs,  $b$  is the length of

long axis of the ellipsoid and the distance between the centers of two ellipsoids, and  $N_{\perp}$  and  $N_{\parallel}$  are demagnetization factors of the ellipsoid parallel and perpendicular to the axis of the NWs which depend on the aspect ratio of the ellipsoid. This equation does not show the dependence of  $H_c$  upon inter-pore distance [21]. Eq. (2) can be adopted to explore the present results. According to the equation, if saturation magnetization  $M_s$  increases, the  $H_c$  will increase accordingly. In case of present samples, it is observed that there is an increase in  $H_c$  after MF annealing but this increase is not so large as compare to the increase in  $M_s$  because  $H_c$  also depends on demagnetizing factor and aspect ratio, according to Eq. (2). Due to external applied field there would be alignment of magnetic moments or production of ordered atomic pairs of unlike atoms along the direction of external applied field [12,20]. This phenomenon affects the demagnetization factor thus resulting in the small increase in  $H_c$  values (as compare to  $M_s$ ). Furthermore, after MF annealing the decrease in the value of  $H_s$  along with an increase in the value of  $SQ$  for  $\text{Co}_{90}\text{Pt}_{10}$  NW arrays is in agreement with the enhanced MA. The NW samples are then reannealed in the absence of magnetic field at  $600^\circ\text{C}$  to erase the effect of MF annealing and to find the actual cause of enhanced magnetic anisotropy. Reannealing of the samples does not completely remove the enhanced anisotropy. The relative change in  $M_s$ ,  $H_c$ , and  $SQ$  values for CoPt nanowires after reannealing as compared with those obtained after MF annealing is very small. This small change can be interpreted because of change in grain size at high temperatures but that change is limited due to the shape of NW samples.

For the structure and phase evaluation of aligned  $\text{Co}_{90}\text{Pt}_{10}$  and Co NWs, XRD patterns are taken before, after MF annealing and reannealing. For these measurements, the Al substrates are etched away by an amalgamation process using a saturated  $\text{HgCl}_2$  aqueous solution and washed thoroughly with distilled water. X-ray diffraction patterns in Fig. 5 show that both  $\text{Co}_{90}\text{Pt}_{10}$  and Co NWs are mainly crystallized in the fcc structure with (111) preferred orientation. The fcc phase of  $\text{Co}_{90}\text{Pt}_{10}$  NWs is dominant in as-deposited state with (111), (200) and (110) reflections. The major phase, in this state, is orientated along (111) reflection which is along the axis of the NWs. After MF annealing the fcc structure and the preferred (111) orientation are preserved as shown in Fig. 5(a). Since the magnetic field is applied parallel to the NW axis during annealing, therefore more crystal grains are expected to have their easy axis of magnetization parallel to the NW axis that is also obvious from the increase in the intensity of more prominent peak along the NW. Texture analysis indicates

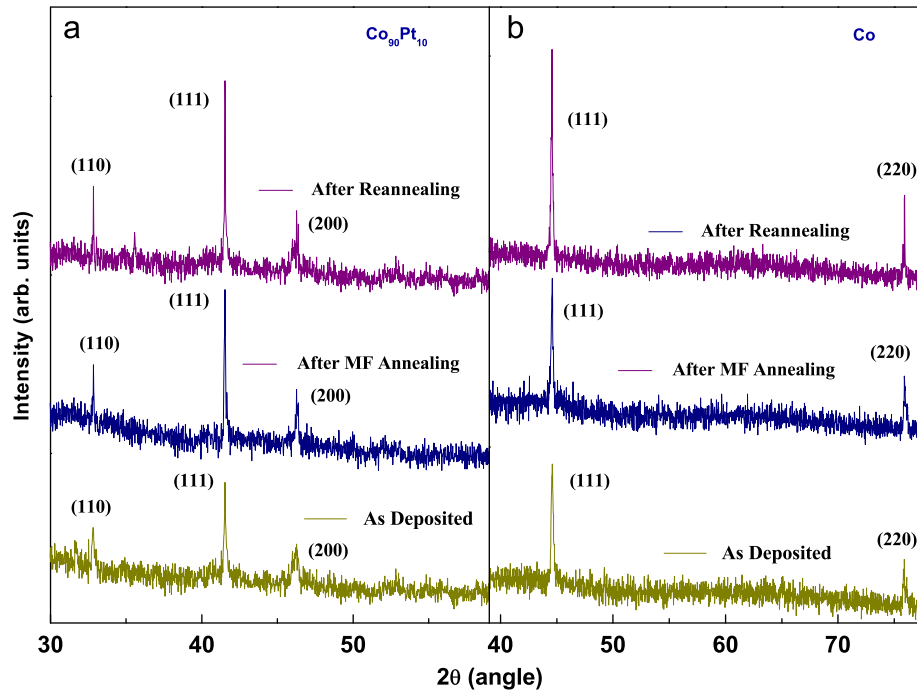


Fig. 5. XRD patterns of aligned (a)  $\text{Co}_{90}\text{Pt}_{10}$  nanowires and (b) Co nanowires, in the AAO template before and after MF annealing and reannealing.

that MF annealing does improve the orientation distribution of crystals in the CoPt samples indicating the alignment of domains along the magnetic field without any phase transformation. The XRD patterns of Co NWs show the characteristic diffraction patterns arising from fcc phase corresponding to (111) and (220). Hexagonal close packing (hcp) is the usual structure for electroplated cobalt. However, the fcc cobalt can be obtained from electrodeposition at ambient temperature by varying the deposition conditions. In the present experiment, low pH value ( $\sim 3.0$ ) [20] of the electrolyte has been adopted to get fcc structure. The as-deposited sample and the annealed samples have fcc structure and preferred (111) orientation along the axis of the wire. The XRD patterns for Co NWs remain unchanged after MF annealing. However, after  $600^\circ\text{C}$  reannealing the intensity of peaks increases due to the crystallization process. From the results of XRD and observation of microstructure, no phase change has been observed which predicts that the magnetic anisotropy of CoPt NWs is enhanced by the atomic pair ordering of Co and Pt atoms.

Fig. 6 shows the magnetic hysteresis loop of  $\text{Co}_{90}\text{Pt}_{10}$  NWs as deposited, after 2 h annealing in zero MF at  $500^\circ\text{C}$  and after 2 h MF annealing at  $265^\circ\text{C}$ . Significant changes in magnetic properties have been observed after MF annealing at  $265^\circ\text{C}$  compared to annealing without MF at  $500^\circ\text{C}$ . A long period of time and high temperature will be required to produce similar magnetic changes by the process of annealing without magnetic field [17].

The MF annealing has affected the magnetic features by minimizing the magnetic anisotropy energy of the system due to the stress relief between grains and directional atomic pair ordering. The direction of bonds of dissimilar atoms (Co, Pt) of the samples may take on an asymmetric distribution if magnetic field, temperature and time for the annealing are sufficient [12]. Furthermore, the MF annealing decreases the dipole magnetostatic interactions and self-demagnetizing fields of the wires due to redistribution of pair directions perpendicular to magnetization in each domain. This redistribution causes a large increase in the values of  $M_s$ . The reason for persistence of enhanced anisotropy after reannealing at  $600^\circ\text{C}$  is related to some structural source like

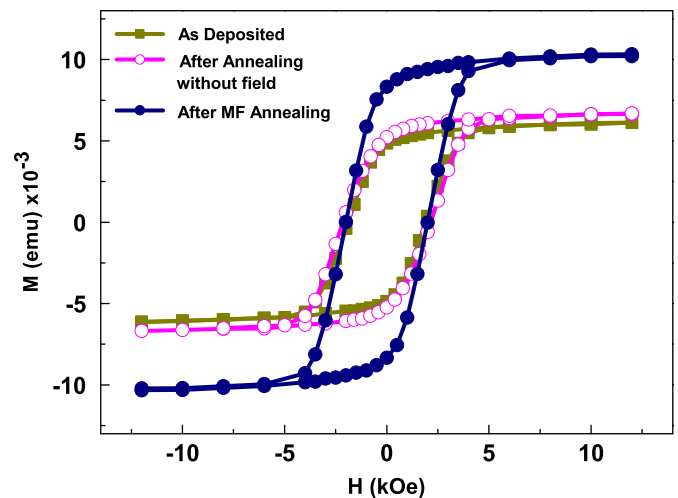


Fig. 6. Magnetic hysteresis curves of  $\text{Co}_{90}\text{Pt}_{10}$  alloy nanowire arrays measured with magnetic field applied parallel to the nanowire axis as deposited, after annealing without MF and after MF annealing process.

shape of the nanowires and preferred crystalline orientations. Alignment of the grains and the magnetic anisotropy may be further enhanced if the CoPt samples are annealed in the high magnetic field for a longer period of time. The present work provides a comprehensive study of the magnetic field annealing dependent magnetic properties of  $\text{Co}_{90}\text{Pt}_{10}$  alloy NW arrays.

#### 4. Conclusions

The magnetic and microstructural behaviors of  $\text{Co}_{90}\text{Pt}_{10}$  alloy NWs and Co NWs are investigated before annealing, after MF annealing and then reannealing of the samples. The results presented here have been explained on the basis of model of prolate ellipsoidal chains. The magnetic anisotropy has been

enhanced in Co<sub>90</sub>Pt<sub>10</sub> alloy NWs by MF annealing which persists after reannealing at higher temperature without field. Co NW arrays do not show response to the MF annealing treatment. It is concluded that the enhanced anisotropy, originated from diffusional atomic pair ordering of unlike atoms aligned with magnetic field, and structural source (shape of the NWs) can influence the magnetic properties of the NWs. After reannealing at 600 °C, no significant change in magnetic properties reveals that major role in persistence of enhanced anisotropy is played by shape of the NWs. In conclusion, we have demonstrated that the magnetic anisotropy can be enhanced in alloy NWs by applying magnetic field annealing.

### Acknowledgments

This research was supported by the State Key Project of Fundamental Research, Ministry of Science and Technology (MOST, Grant no. 2006CB932200), and Chinese National Natural Science Foundation (NSFC, Grant nos. 10574156, 50528101 and 50721001).

### References

- [1] L. Wuxia, Y. Peng, J. Zhang, G.A. Jones, T.H. Shen, J. Phys. Conf. Ser. 17 (2005) 20.
- [2] Y. Dahmane, L. Cagnon, J. Voiron, S. Pairis, M. Bacia, L. Ortega, N. Benbrahim, A. Kadri, J. Phys. D 39 (2006) 4523.
- [3] J. Mallet, K. Yu-Zhang, C.L. Chien, T.S. Eagleton, P.C. Searson, Appl. Phys. Lett. 84 (2004) 3900.
- [4] S. Franz, P.L. Cavallotti, M. Bestetti, V. Sirtori, L. Lombardi, J. Magn. Mater. 272 (2004) 2430.
- [5] T.R. Gao, L.F. Yin, C.S. Tian, M. Lu, H. Sang, S.M. Zhou, J. Magn. Mater. 300 (2006) 471.
- [6] G.C. Han, B.Y. Zong, P. Luo, Y.H. Wu, J. Appl. Phys. 93 (2003) 9202.
- [7] A.I. Gapin, X.R. Ye, J.F. Aubuchon, L.H. Chen, Y.J. Tang, S. Jin, J. Appl. Phys. 99 (2006) 08G902.
- [8] S. Chatman, A.J.G. Noel, K.M. Poduska, J. Appl. Phys. 98 (2005) 113902.
- [9] S. Shamaila, R. Sharif, S. Riaz, M. Ma, M. Khaleeq-ur-Rahman, X.F. Han, J. Magn. Mater. 320 (2008).
- [10] J. Mallet, K. Yu-Zhang, S. Matefi-Tempfli, M. Matefi-Tempfli, L. Piroux, J. Phys. D 38 (2005) 909.
- [11] H. Zeng, R. Skomski, L. Menon, Y. Liu, S. Bandyopadhyay, D.J. Sellmyer, Phys. Rev. B 65 (2002) 134426.
- [12] R.C. OHandley, Modern Magnetic Materials: Principal and Applications, Wiley, New York, 2000.
- [13] S.H. Ge, X. Ma, C. Li, W. Li, J. Magn. Mater. 226–230 (2001) 1867.
- [14] J. Sa'nchez-Barriga, M. Lucas, G. Rivero, P. Marin, A. Hernando, J. Magn. Mater. 312 (2007) 99.
- [15] J.U. Cho, J.-H. Wu, J.H. Min, J.H. Lee, H.-L. Liu, Y.K. Kim, J. Magn. Mater. 310 (2007) 2420.
- [16] F. Johnson, H. Garmestani, S.Y. Chu, M.E. McHenry, D.E. Laughlin, IEEE Trans. Magn. 40 (2004) 2697.
- [17] D.S. Lia, H. Garmestania, S.-s. Yanb, M. Elkawnic, M.B. Bacaltchukc, H.J. Schneider-Muntauc, J.P. Liud, S. Sahae, J.A. Barnard, J. Magn. Mater. 281 (2004) 272.
- [18] Y. Yoshizawa, K. Yamauchi, IEEE Trans. Magn. 25 (1989) 3324.
- [19] F. Johnson, C.Y. Um, M.E. McHenry, H. Garmestani, J. Magn. Mater. 297 (2006) 93.
- [20] A. Encinas, M. Demand, J.-M. George, L. Piroux, IEEE Trans. Magn. 38 (2002) 2574.
- [21] H.L. Su, G.B. Ji, S.L. Tang, Z. Li, B.X. Gu, Y.W. Du, Nanotechnology 16 (2005) 429.